Bridge Structures 7 (2011) 3–18
DOI:10.3233/BRS-2011-015
IOS Press

I35W Bridge collapse: Lessons learned and challenges revealed

S. Hao
ACII, INC. P.O. Box 8090, Wilmette, IL 60091-8090, USA
Tel.: +1 847 920 9475; Fax: +1 847 256 3014; E-mail: hao0@suhao-acii.co

Abstract. This article discusses issues of structural design revealed by the collapse of I35W Bridge on August 1st, 2007. The article is based on analysis of the original bridge design drawings, a series of detailed finite elements computations, and material evidence disclosed by National Safety Transportation Safety Board (NTSB) official investigation. These issues include (i) redundancy considerations for multi-span bridge; (ii) reason for under-designed bridge elements; (iii) effects of lateral force on gusset plates' load capacity in a steel-truss structure; (iv) criterion of gusset plate's stability and thin-plate theory-based model for load-rating. This analysis concludes that the lessons learned from the I35W Bridge collapse may have certain significance for the safety assessments of similar steel bridges. According to recent surveys, there are scores of this kind of aged bridges that are still in service [38, 41].

1. Introduction

The past century can be remembered as the most successful period for bridge engineering, which has also brought up great challenges to bridge engineers to digest rapidly-developed ideas, new tools, and novel methodologies in related engineering sciences while to assure new designs and existing bridges' operation being safe, economic, and technologically advancing. While enjoying great success for decades, we did have suffered several significant setbacks. One example is the collapse of the Minneapolis I35W highway bridge.

August 1st of 2007, 6:05PM, the interstate I35W Bridge in the City Minneapolis, Minnesota, collapsed suddenly. The 8 traffic-lane, 1000-foot-long deck of the 1907-foot-long bridge fell into Mississippi River within seconds, resulted in 13 fatalities and 145 injuries, see Figs 1 and 2.

Designed in 1964 and opened to traffic at 1967, the I35W Bridge stretches from north to south over the Mississippi River in the City Minneapolis in Hennepin County, Minnesota. The major part of the bridge is a 1000 foot (304.8 meters) long, 108 foot (32.92 meters) wide, three-span steel deck-truss superstructure, which collapsed completely. The bridge originally had six traffic lanes. After two major rehabs in last century, it has been widened into eight lanes with two auxiliary lanes and its concrete deck has been reinforced from 6.5 inches to 8.5 inches thick. NTSB's official investigation [34, 35] indicates that, at the moment of the collapse, two lanes of the bridge were occupied by piled construction materials and heavy trucks; four lanes were opened to traffic; and the other two lanes were empty.

This article summarizes an independent investigation of this disaster based on material evidences and advanced computations. The theoretical background and the analytical methodologies applied can be found, for examples, those in the references list [2–4, 6–8, 10, 17, 20, 21, 24–27, 29, 30–33, 36, 37, 39, 40, 42–49, 52]. A part of preliminary results of this analysis have been submitted to the related investigation and administrative agencies since the second week after the bridge's collapse [14–16].

This article is organized as follows: The next section introduces the structural and material's models applied in the analysis. The third section analyzes the results obtained and compares the data with materials' evidences. The following section discusses the reasons that had caused this bridge's undersized design. The fifth section explores further the underlying struc-

Fig. 1. Minneapolis I35 W Bridge: Before and after the collapse. (a) The I35 W bridge (right) at 1970. (b) August 2nd, 2007.

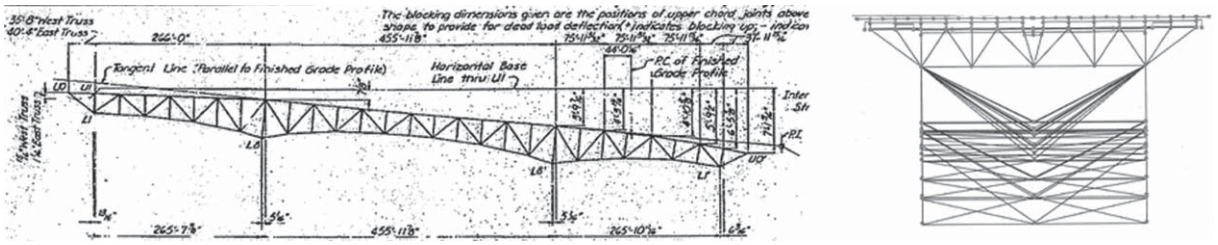

(a) (b)

Fig. 2. Layout of the superstructure: (a) main frame; (b) lateral bracings and floor trusses.

tural issues that triggered the collapse, from which the lessons learned do have certain significance for the procedure of gusset plates' assessment currently applied. A model based on two-dimensional plate buckling theory has been introduced. The last section summarizes the conclusions.

2. Methodology and model applied

2.1. Structural model

As depicted in Fig. 2, the steel superstructure of I35W Bridge contains three parts: (i) two main truss-frames, west and east; (ii) lateral bracings and 27 floor trusses, (iii) reinforced concrete-slab deck. Figure 3 is a two-dimensional model of the bridge's main frame and the locations of major gusset plates, i.e. the nodes in the truss-network. Additional subscript "*E*" or "*W*" may be used in the following text to denote a node at eastern or western main frame. As illustrated in Fig. 4a, a two-level computational model has been developed, i.e. using 3D finite element to obtain force-deflection behavior of gusset plate, which is implemented into truss network of the bridge superstructure.

2.2. Materials model

A structural failure is often started by material's failure in one or several key-structural components, which introduces extra complexities to an analysis of a structural collapse like I35W Bridge. In a new sustainable structure's design, it is generally required to keep the stress level in all components within material's yield limit. By contrast, a failure means applied stress reaches a material's strength limit while the material's strain surpasses yield strain. As explained by the example in Fig. 4b, for the defect-free plate under uniaxial tension on left-upper corner, the corresponding average stress-strain curve is the solid line that linearly increases from the origin and connects the thick dash line that ascends nonlinearly, plotted in middle. A material's failure is

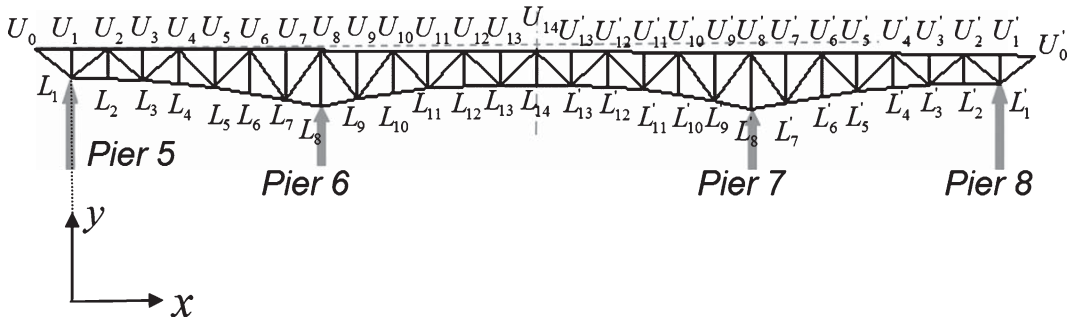

Fig. 3. Nodes and support piers of the main truss frame, where U and L stand for the nodes on upper and lower chords, respectively; a prime is attached to denote the nodes in south half span (right).

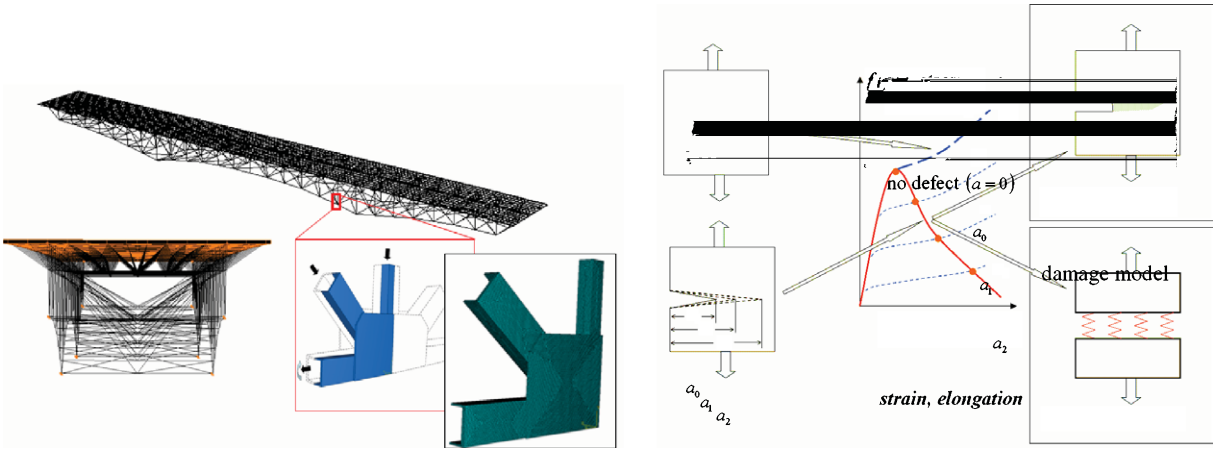

(a) (b)

Fig. 4. (a) A two-level 3D FE Models of the bridge; (b) Model to represent a material failure, e.g. damage-induced-crack, resulted structural failure.

the result of evolution of one or many defects. When a defect in the form of crack exists in the plate, as plotted in the lower-left, the average stress-strain relations can be represented by the linearly solid line connected with these thin short-dashed lines corresponding for different crack lengths. When the material elements at crack tip fails, the crack grows, for example, from a_0 to a_2, the plate's elongation will increase continuously while applied stress decreases, as illustrated by the solid line connected through the dots. For common 30–50 grade mild structural steels at room temperature, such a crack growth is an accumulation of micro-scaled damages in the form of voids nucleation, growth and coalescence [10, 25, 29, 30, 37, 42–44, 49]. The "spring model" or "cohesive model", developed in [37, 42], have been implemented into finite element analysis to count such a damage-induced material's failure.

2.3. Cases analyzed

In the first report that was finished seven weeks after the disaster [14], a primary object was to identify the locations that might initiate the failure through computer simulations of various possible failure processes, so as to assist official investigation to identify the actual location and causes. Due to limited data and information at the time, 2D and 3D computer simulations for about 20 cases of the bridge's superstructure's failure have been performed to consider various circumstances which include (a) the effects of supporting bearing conditions to superstructure's load path and stress amplitude; (b) whether the bridge-deck's slop (about 1 degree, see Fig. 2) caused extra horizontal forces; (c) temperature's change-induced thermal stresses, which include two cases: day-night and sea-

sonal shifts caused uniform changes and the case with non-uniform temperature distribution, for example, the upper chords (the trusses near deck) are warmer than other parts; (d) pre-existing defects at various locations; see Fig. 5. In all of these computations, uniformly distributed deck load and the weight of trusses members are accounted as live and dead load, respectively.

3. Results and discussion

3.1. Forces and bending moments distributions

Plotted in Fig. 6(a) are the uniaxial forces in the four groups of truss members in main frame, which are upper chords, lower chords, truss diagonals, and truss verticals. The force in upper chords, the solid line connecting small solid dots, reaches its positive maximum above the piers of center span while the negative maximum at the center. By contrast, the force in lower chords, the light dash-dot line, has a positive peak at the center and two negative maximums above the piers. The distribution of the force in truss diagonals (solid line) is characterized by the peaks around the spots where the upper chord's force decreases from positive to negative while the lower chord's force inversely uprises. As plotted in Fig. 6(b), the bending moment in truss-verticals is ignorable whereas that in other reaches positive maximum in the centre of middle span and negative maximum just above two piers. In this case the bending moment in the diagonal members is generally lower than that in upper and lower chords.

Figure 7a shows a comparison of the upper chords' uniaxial forces for the cases 0, 1, 2, and 5, which indicates that the deck's slope and the horizontal constraint/forces from approaching spans do not have remarkable effects on this force's distribution. By contrast, Fig. 7(b) are the bending moments in upper chords when temperature changes while supporting bearings are locked, i.e. the cases 3 and case 4 in Fig. 5, respectively; compared with the case 2 that is the normal design condition. It demonstrates a significant combined effect of temperature change and locked bearing. In practice, severe corrosion may drastically increase the friction resistance of a bridge's roller bearing; an extreme case is that a roller bearing eventually is fully locked so it becomes a pin point that does not allow horizontal movement. This induces considerable high

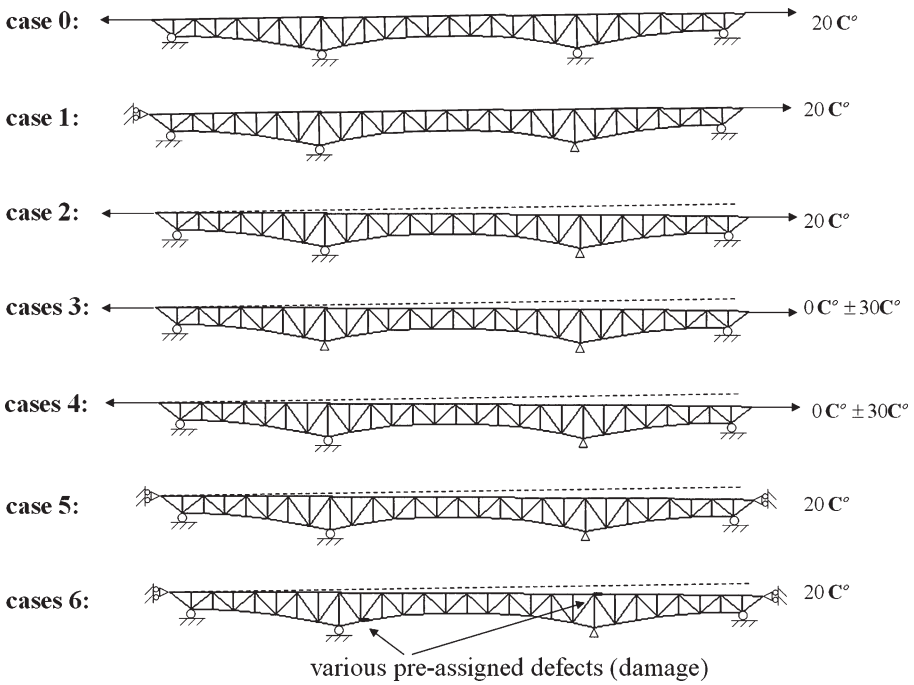

Fig. 5. Case 0 : no deck-slop and all bearing assumed to be rollers; case 1 : the same as 0 but the bearing above pier 7 was locked; case 2 : design condition - the same as 1 but with deck slope; case 3 : design condition but with locked bearing above pier 6 under different temperatures; case 4 : design condition but under various temperatures; case 5 : design condition but assuming no horizontal elongation; case 6 : design condition but with pre-existing defects at various gusset plates locations; see [14]. Each case contains several respective sub-cases with different parameters.

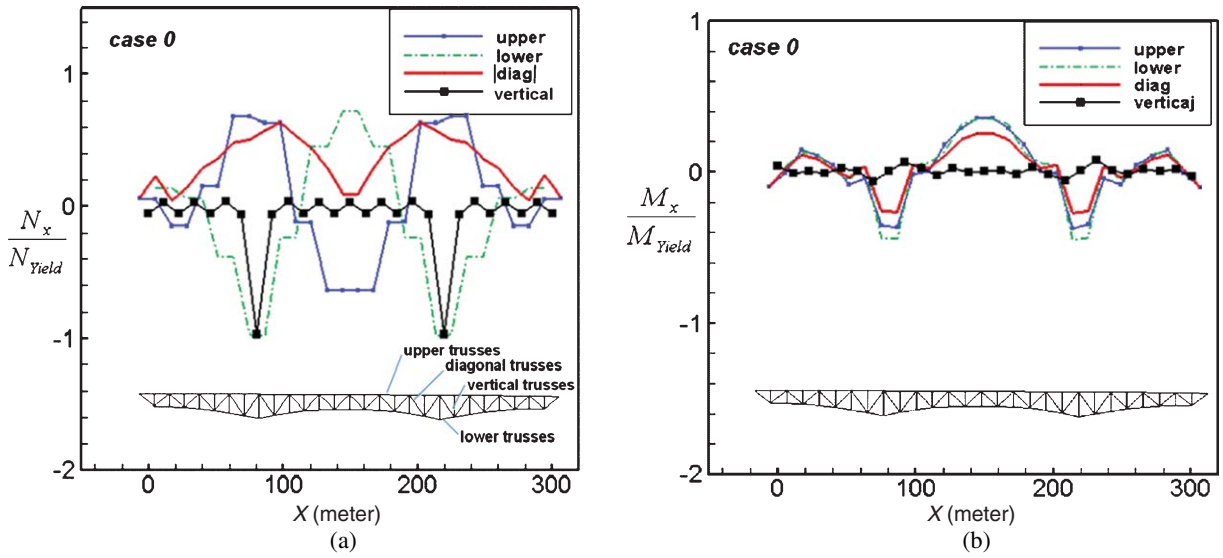

Fig. 6. (a) Uniaxial force in the four groups of major truss members in main frame, where N_x is the uniaxial force and N_{Yield} is that when material yields; (b) the bending moment distributions, where M_x is in-plane moment and M_{Yield} is the moment at yield. No bearing-lock or temperature change (case 0).

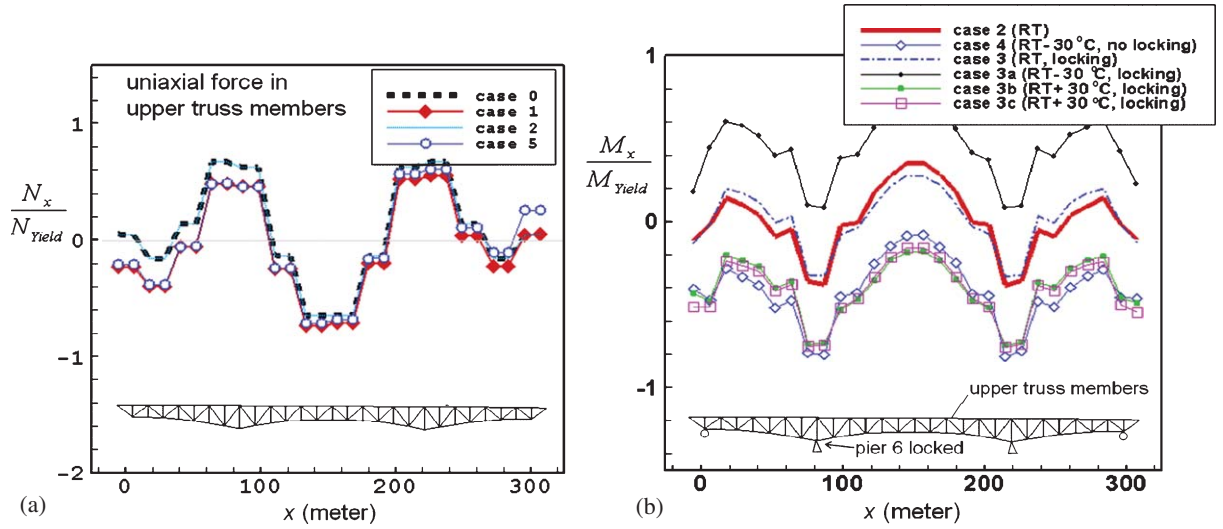

Fig. 7. The same plots as that in Fig. 6 but considering temperature change and locked bearings, where RT refers to room temperature; (a) Uniaxial forces in upper chords and (b) the corresponding bending moment.

thermal stress when temperature changes, as demonstrated by this plot.

3.2. Scenario of the collapse

Now we discuss the following two issues: The sequence of the bridge's superstructure's collapse and what we can learn from it. One may notice that the force and bending moment distributions in Figs 6 and 7 are nearly symmetric to the central span of the bridge. Just after the disaster, there was an argument regarding the sequence of the failure, i.e., which approach of the bridge failed first. An opinion gained many echoes was that all structural components between the two piers over the river failed almost simultaneously, i.e. a horizontal fall of the central span. To clarify this

Fig. 8. The scenario of the progressive collapse presented by I35 W (Army Corps' Video).

issue, Fig. 8 are the photographic pictures recorded by Army Engr. Corp. from south side of the bridge, which was reported by medium (CNN). The water splashes at the moment that middle span was fallen, i.e. Fig. 8(d), reveals the collapse initiated from south side [14]. The north approach span failed subsequently without showing any capacity to resist the collapse.

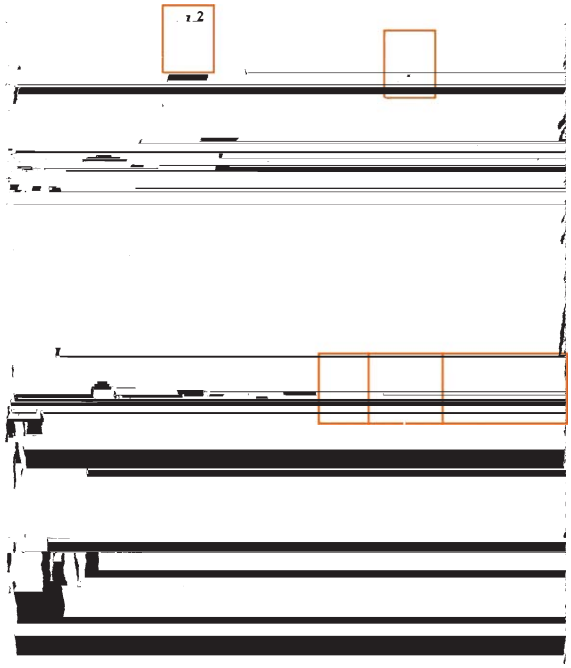

Fig. 9. The influence-line solutions explain the benefit of a three-span bridge's design like that in I35 W because the peak bending moment in case (c) is much lower than that in case (a) and case (b) for the same span length "*b*" and uniformly distributed load density "*q*".

In bridge design, the three-span like I35W is a common structure; the underlying idea is to gain long central span with minimized cost. This can be explained by the influence-line solutions in Fig. 9. By comparing the bending moments in the three cases with the same middle span length "b" and under the same distributed load "q", one can find that the maximum bending moment of the case (a) is about 80% higher than that in case (c); similarly, the moment of case (b) is about 20% higher than case (c).

However, from the viewpoint of structural integrity, the advantage of the three-span design (c) is traded-off by lower redundancy. This is because, when one of three spans is severely damaged or fails, the force distributions in other two shift back to the situation similar to the case (a). Such a scenario is illustrated in Fig. 10. This, the author believes, was a reason that caused the progressive collapse of I35W Bridge. This leads to a conclusion that states as following: to avoid a similar progressive collapse that occurred in I35W Bridge, an additional safety factor may be necessary for those key single-load path structural components in a multi-span bridge if its design of load capacity is

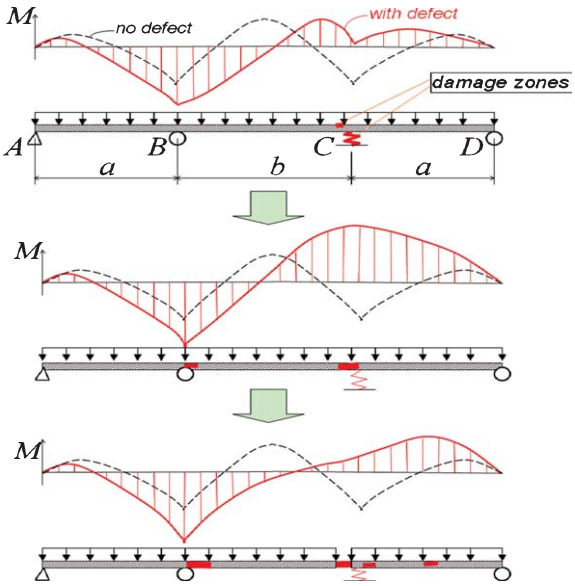

Fig. 10. A scenario that a material's failure induces a progressive structural failure in a three-span bridge, where the material's failure occurs first at the location just above the bearing support C, which results in the material's failure around the bearing support B; subsequently the beam AB becomes a simple span that is the same as the case (a) in Fig. 9.

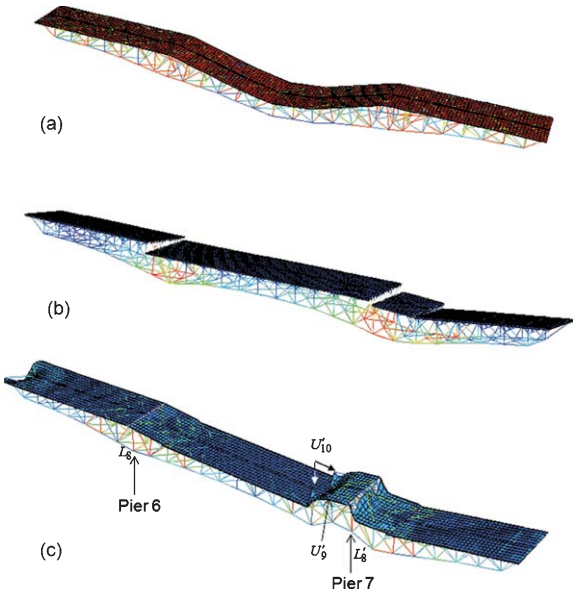

Fig. 11. Three failure patterns of the bridge.

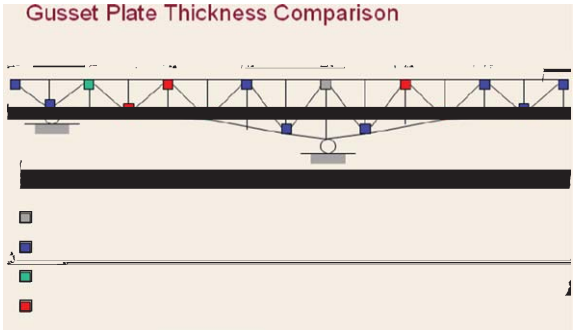

Fig. 12. Gusset Plates Thickness in I35 W Bridge [22, 35].

merely based on the influence-line analysis described in Fig. 9(c).

3.3. Where the collapse started

The early study [14] suggested that damage-induced material's failure caused the structural failure. Such a material's damage can be, for example, fatigue-induced cracks or significant corrosion-resulted section loss. Obviously, an undersized design has the same effect as such a damge. Three possible failure patterns were focused, see Fig. 11, and the case (c) was considered as mostly close to reality [14]. Although this simulation was done just a couple of weeks after the collapse (submitted to NTSB at August 17th, 2007), it does demonstrate significant deflection around the node U'9 and U'10. The "undersized" gusset plate U'10 actually initiated the bridge's failure [22, 34, 35].

3.4. NTSB's findings and conclusions

After thorough examination of the wrecked pieces of the bridge, at January 15, 2008 and November of 2008, respectively, NTSB has released the results of the official investigation [22, 35], which disclosed that the gusset plates at the nodes U10, U'10, L11, L'11 in main frames of central span and U4, L3, U'4, L'3 of the approach-spans are undersized, which are half inch thick.

By contract, all other gusset plates in the nodes that connect four or five truss members were one inch in thickness or more, see Fig. 12. Also, the NTSB's analyses of the video recorded at the instance of the collapse indicates that the half-inched gusset plate at node U'10 failed first, which triggered the subsequent collapse of the bridge. The record of the design firm of the I35W bridge reveals the bridge designed without appropriated calculation, which resulted in the undersized gusset plates.

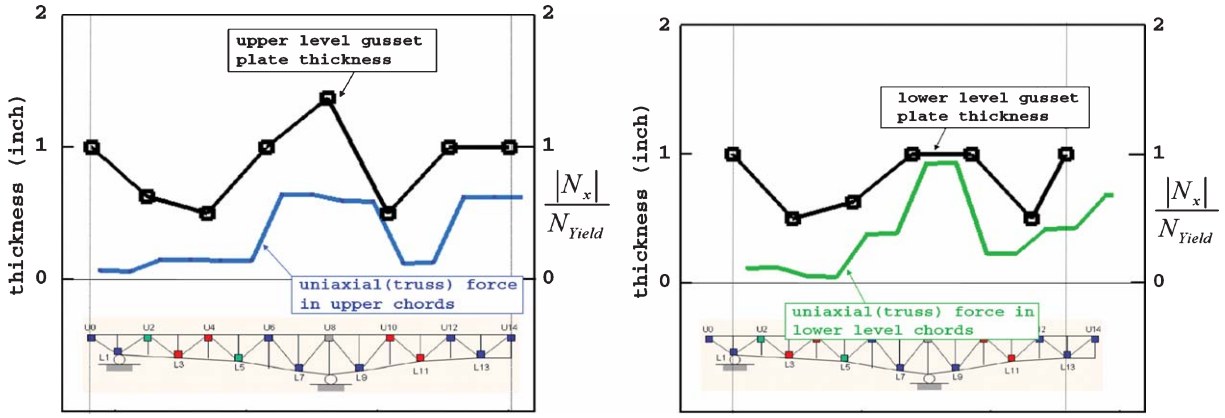

(a) (b)

Fig. 13. Comparisons between the gusset plate thickness and the uniaxial forces in horizontal truss members plotted in Fig. 7 a: (a) upper chords; (b) lower level chords.

4. Why the gusset plates undersized

Plotted in Fig. 13 are the comparisons between the actual gusset thicknesses from Fig. 12 and the uniaxial forces of upper and lower-chards that were given in Fig. 6(a). An obvious coincidences between the force distributions and gusset thicknesses can be seen except near the end nodes (U0, L1). All half-inch gusset plates (U4, U10, L3, L11) are at or close to the locations with the lowest truss force. This fact seems implying that the plates' thicknesses were designed based on the forces in horizontal trusses.

However, by checking the results plotted in Fig. 6(a) carefully, one can find another fact: the force in diagonal member almost reaches its peak value at the location, for example, between U10L9 and U10L11, where the upper and lower chords forces change signs. The reason is obvious: at this location the diagonal truss U10L9 transfers the deck load-induced compression force flow in middle upper chords of central span into lower chords and supporting bearings; whereas U10L11 transfers the tension force flow in middle lower chords into upper chords above the piers; whereby the gusset plates like L9, U10 and L11 are the "pivots" for these load paths of force flows, as explained in Fig. 14.

Therefore, a statement has been given in the third paragraph, section 5 of the report [14]: "Due to the limited computation capability in past, it seems that the original design and subsequent early investigations could only treat the 9340 bridge* as a truss-assembled structure, which led to the focus onto the forces and damage conditions in truss members. . .". Obviously, the truss force in upper and lower level chords had been used as the governing parameters for the gusset plate design, whereas the corresponding stress concentration in the gusset plates did not obtain sufficient consideration at the time.

Based on an examination of all original design drawings and the material evidences disclosed by NTSB's investigation, several other "undersized" structural components have also been identified in the analysis [11]. These components are the upper and lower chords attached to those undersized gusset plates in Fig. 12. It has been found that the thicknesses of upper chords' wall and gusset plates are actually proportional to the bending moment solution of the one-dimensional influence line analysis illustrated in Fig. 10c. This fact reveals that the NTSB-disclosed undersized gusset plates are the consequence of a bias toward a "one-dimensional model" in the original design, which did not give sufficient consideration to the effects of the forces from diagonal truss members input into gusset plates [11].

5. "Truss approximation" and gusset plate

A practical question is: how to determine a gusset plate's capacity in practical applications? Conventional consideration treats gusset plates as additional stiffeners that do not have significant effect to a truss network load capacity. The author of this paper had also been convinced for while that "truss-approximation", i.e.

* The I35W Bridge is numbered as 9340 in national bridge inventory.

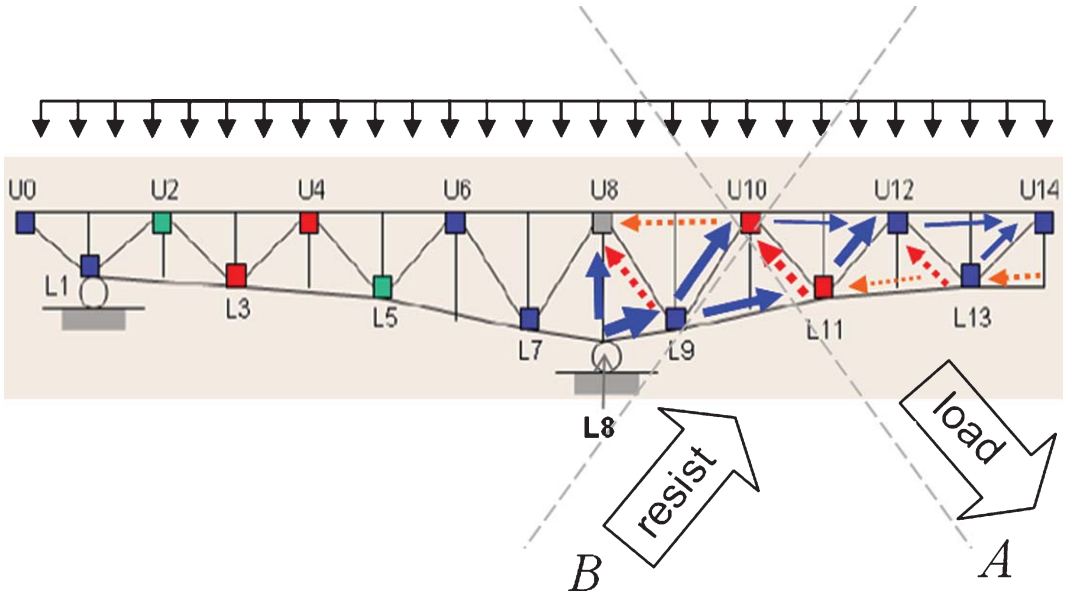

Fig. 14. An illustration of the main "load path" in central span of I35 W, where the blue solid-line arrows represent compression and the red dotted line arrows represent tension. The compression is mainly corresponding to the resistance from the pier and the global bending moment; whereas the tension is mainly corresponding to span's weight and deck load. The gusset plates U10, L11, U12 are the pivots to balance load and resistance forces transferred by diagonal members. The major function of vertical trusses is to provide redundancy to the truss cells except the member L8-U8.

omitting bending moment and shear in slender structural members of a truss network, was good enough for applications. Under this approximation, a gusset, which fastens connected truss-members, becomes a "hinge" that allows free rotation between adjacent members because of no bending moment exists. This approximation generally provides acceptable accuracy for long beams/trusses while significantly simplifies analysis, which has been successfully applied over centuries. However, it should be noticed that the resulted "hinge approximation" implies the ignorance of the secondary stress caused by bending moment at a gusset plate and the corresponding stress concentration. These stresses may not have significant effect to truss members but can be crucial for a gusset plate. To demonstrate this point, two simple examples are given in Fig. 15 to explain the differences.

Figure 15(a) shows a square truss-cell that is unstable when the nodes at the corners are hinges. Adding gusset plates to keep the adjacent trusses perpendicular to each other, which makes the cell becomes a stable frame but results in bending moment at the gusset. When an additional diagonal truss is added to the cell in (a), as illustrated in Fig. 15(b), the cell becomes a stable structure despite hinges at the nodes. The corresponding bending moment in upper chord is plotted when a concentrated force is imposed. As a comparison, the lower part of this figure is an analytical solution when the nodes are stiffened by gusset plates; stronger diagonal member results in higher bending moment at the node, hence, the gusset plate.

It is no doubt that "truss approximation" can provide satisfied solution for the uniaxial forces of slender members in many cases. However, when force flows in a truss-network are not uniform, instead, varying drastically, the corresponding bending moments, particularly, at gusset plates, can be remarkable. This may occur at least under the following three conditions: (i)concentrated load presents; (ii) inhomogeneous internal stress, for example, thermal stress; (iii) residual stresses caused by, for example, in-appropriated welding or cambering. For a structural member like a gusset plate with complicated geometry, a bending moment-induced stresses and corresponding stress concentration may have substantial effects on its load capacity and fatigue life. The effect of bending moment can be viewed directly by the numerical analysis presented in Fig. 9(c), which shows significant relative rotation between adjacent trusses around those pivotal nodes such as U10, L11 when the superstructure starts to fail. This result can be verified by the bowing of the actual U'10 gusset plate observed four years before the

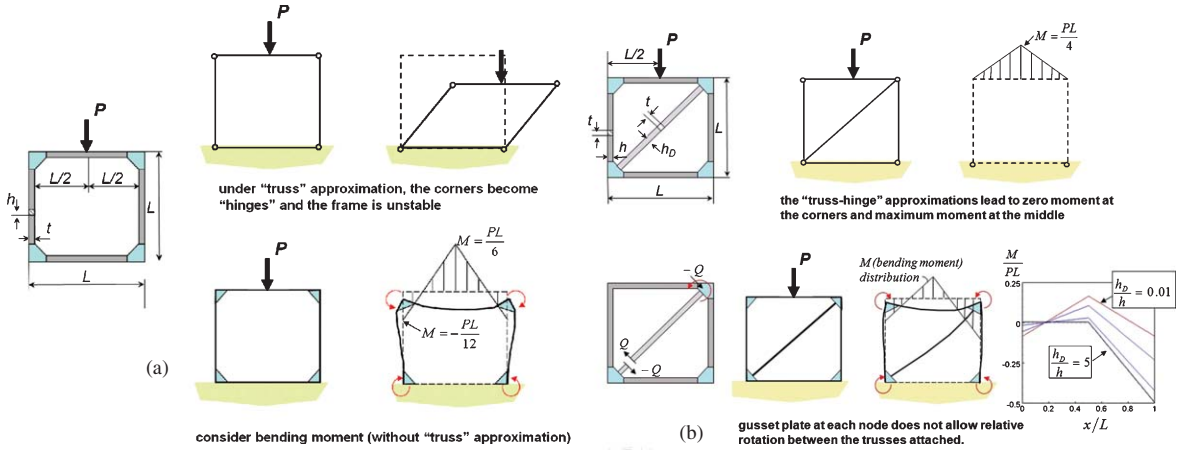

Fig. 15. (a) The truss-cell is an unstable structure when hinges are at the corner. By contrast, gusset plates keep the adjacent trusses perpendicular to each other, resulted in the bending moments at the corners; (b) An additional diagonal bracing stabilizes the frame; the bending moments become more remarkable at the upper-right node gusset and its amplitude increases when the ratio of the widths of diagonal bracing (h_D) and vertical trusses (h) increases; when this ratio is large, the upper horizontal truss is like a cantilever fixed at right end by the gusset plate.

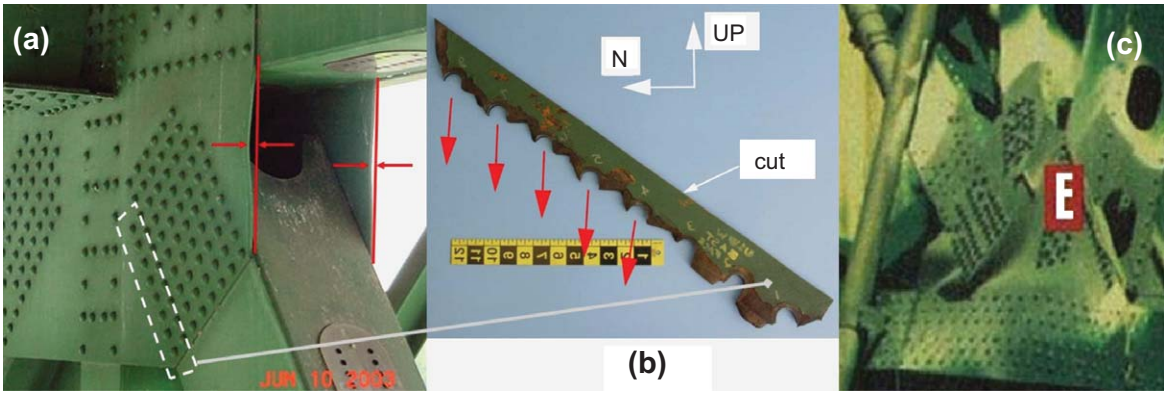

Fig. 16. Three patterns of gussets' failures: (a) bowing, I35 W Bridge's gusset plate U10' [34]; (b) a cut of the U10' plate's lower part; (c) buckling due to the large ratio of unbraced length /gusset thickness, which occurred in the highway I90 Grand River Bridge, Ohio, 1997 [23].

bridge's collapse, see Fig. 16(a), which could be caused by a past deck's overload or the result of cambering during erection. In either case, such a bowing implies reduction of the gusset's load capacity and, thus, its vulnerability to this kind of loads applied later.

6. Gusset plates' load rating

6.1. Failure patterns of gusset plates

The gusset plates' failure in I35W Bridge is not a unique case. Figure 16(c) shows a gusset's buckling that occurred 1997 at the Grand River Bridge that carried highway I90 of Ohio [1, 23]. Therefore, it can be assure that gusset plate may fail at least by three different patterns: (i) bending and associated rotation-induced bowing, on the part of a gusset plate with free-edge between two adjacent trusses, see Fig. 16(a); (ii) tension-dominated ductile failure between the edges of two adjacent trusses, which can be a cause or the result of a bowing presented at another edge of one truss, or occurs independently; (iii) buckling in the unbraced area in the front of an attached truss, which may be accompanied by bowing nearby, as demonstrated in Fig. 16(c).

Most gusset plates in steel bridges are made of 30–70 grade mild steels. This class of steels often fails in the

form of ductile fracture except under some particular circumstances such as temperature below ductile-brittle transition point or within the area near or at a welded joint. For a thin gusset plate, buckling or bowing is when compression force reaches instability limit when applied stress may be much lower than yield strength. By contrast, a tension-dominated failure is an accumulation of shear deformation along slip-planes of polycrystalline matrix at yield limit, which may present in two modes: the out-plane shear that induces necking; and the in-plane shear that often starts at a free edge with stress concentration, for example, a rivet's hole or a crack, and then leads to a Lude's band. Both modes present in Fig. 16(b) but within different areas.

6.2. *Load-rating gusset plates*

The "bowing" of the U'10 gusset plate of I35W in Fig. 16a is considered as an early warning sign. That tragedy proofs a failure of such a gusset can lead to entire bridge's fall. Therefore, in a new truss-bridge's design or an aged bridge's load-rating, a practical issue is to identify its load capacity based on each structural components' capacities including all gusset plates, whereby the following two steps are essential

1) Compute the forces and bending moments input into a gusset plate in a truss bridge, when the "truss approximation" applies, it should be aware of the corresponding deviation in result.
2) Determine the limit state for each gusset plate within engineering acceptable accuracy.

To this end, a procedure and associated computer programs have developed to investigate the failure process of I35W Bridge based on the theories and methodologies introduced in [2–4, 6–8, 10, 17, 20, 21, 24–27, 29, 30–33, 36, 37, 39, 40, 42–49, 52]. A series of in-depth three-dimensional computations of I35W Bridge under the actual live loads at the instance of collapse, see Fig. 17, as well as the bridge under various design conditions, have been performed [11, 15] according to original design drawings and in the light of the material evidences of NTSB's investigation[34, 35] and FHWA's technical advisory [9].

In addition to the discussions of more undersized-components disclosed from original design drawings and the evidence of the one-dimensional influence line solution-biased original design, another conclusion obtained in [11] is that the nodes connecting floor trusses and main truss-frame, see Fig. 17b, was inappropriately designed. This is because it actually divides deck load to two high-amplitude force flows input into a weak gusset plate, i.e. compression on the plate's top and downward tension on its bottom edge. The particular structural features presented in this part and the implications to load capacity are to be discussed in follows because they can be useful for other gusset plates' load rating in general.

Plotted in Fig. 18 are the computed uniaxial stress in the floor trusses that connected the south U10' and

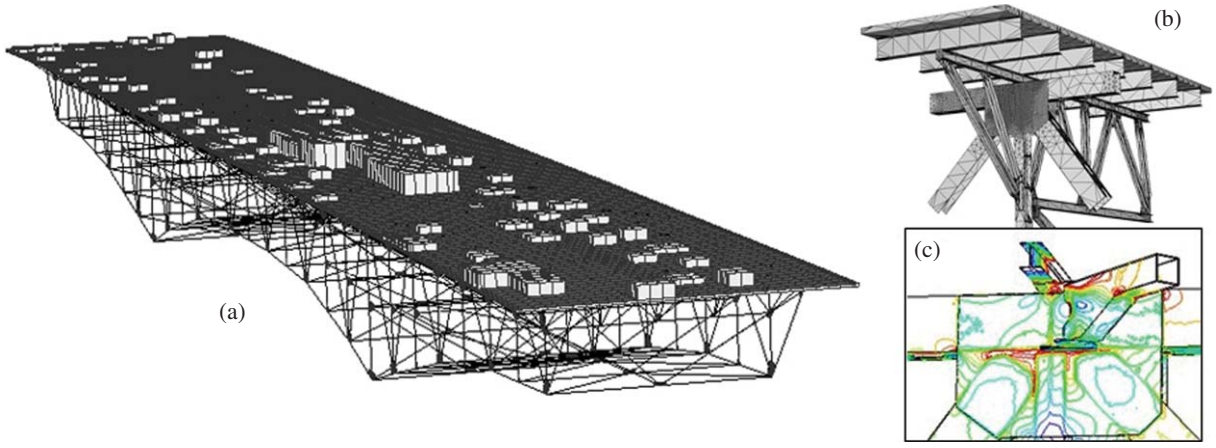

Fig. 17. (a) A fully-scaled computation of I35 W Bridge [7] based on design drawings and live load at the time of collapse, where the trucks, cars, and construction materials are represented by the brick elements with the densities corresponding to their weights; (b) a finite element model for the connection between floor truss and main flame at the node U10; (c) computed stress contour on an inside gusset plate [16], which indicates the stress on the inside horizontal lateral bracing introduces lateral force that affects the deformation of the gusset plate.

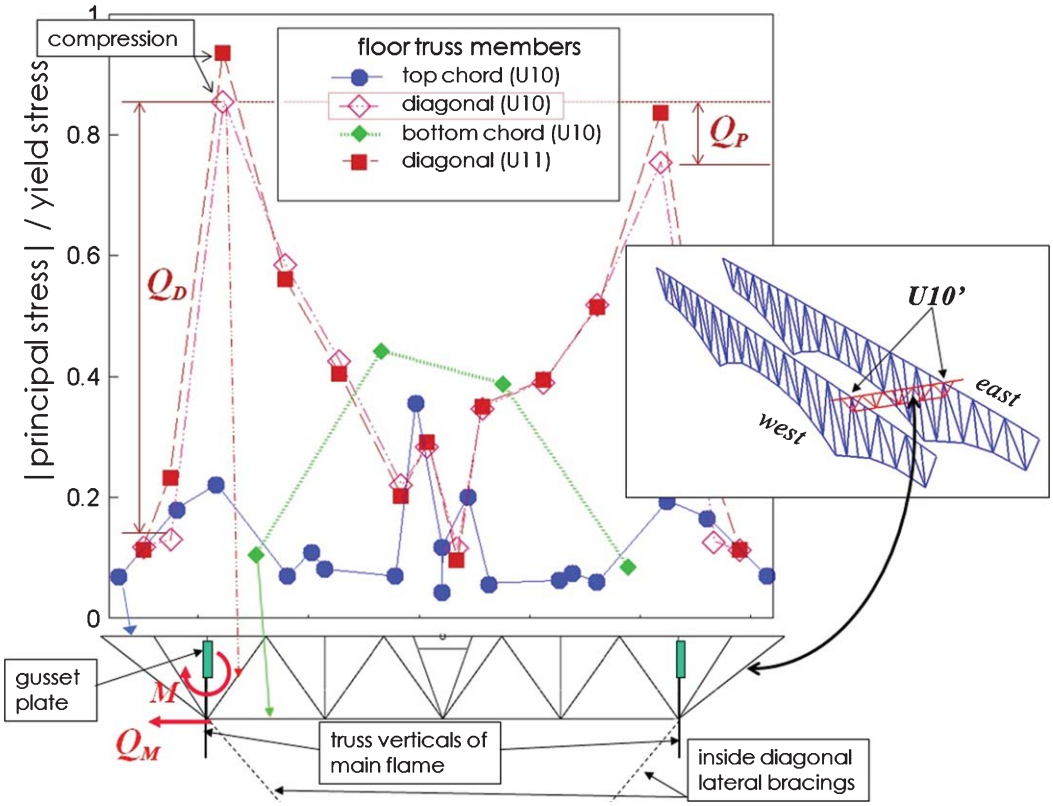

Fig. 18. Stress distribution in floor trusses connect to U10' and U11', which result in the out-of-plane force Q_M and bending moment M onto the gusset plate; see the discussion in the text.

U11' gusset plates of I35W. Here we focus on the stress distribution in the diagonal members of the floor truss attached to U10', which is plotted as the empty diamonds linked by dash lines. One may notice that the two highest stress peaks occur in the diagonal floor truss members just inside the gusset plate on each side, by which the amplitude of the peak near western U10' is about 13% higher than that near the eastern U10'. This difference is denoted as Qp in the figure, which, obviously, is caused by the eccentric deck live load at the moment of the collapse, see Fig. 19a. Another notable phenomenon in Fig. 18 is the difference in stress level between the diagonal floor trusses member inside and outside a gusset. On the western side, it is denoted as Q_D. Because all floor truss diagonals are made of the similar sized H-beams, therefore, the magnitude of Q_D means the force that inside diagonal input to the node below the gusset plate is about 2.6 time higher than the sum of the forces from two outside diagonal members.

Obviously, the difference Q_D reflects the unbalance of the forces at the node that connects main flame's vertical truss, the diagonals and lower (bottom) chord in floor truss. Its horizontal resultant must be balanced by the tensions shared by the bottom chord, the diagonal lateral bracing, and the lateral shear in the main flame vertical truss. According to Fig. 18 there is no significant stress in the bottom chord; whereas the inside diagonal lateral bracing is a very slender beam that has very limited capacity to carry horizontal force. Therefore, the majority of the horizontal force induced by the inside floor truss diagonal is balanced by the lateral shear of the main flame's truss vertical, which is denoted as Q_M in the figure. Q_M produces a bending moment to the attached gusset plate, denoted as M.

On the other hand, the Q_P in Fig. 18 represents the difference of the forces that the floor truss input to eastern and western main flames, respectively. Again, because the stresses on the two ends of floor truss' horizontal members attached to the two main flames are almost equal, Q_P should be balanced by the lateral shear on main truss vertical and the horizontal lateral bracings of two main flames, i.e. the top horizontal lateral bracing attached to gusset plate, as illustrated in Fig. 17(c).

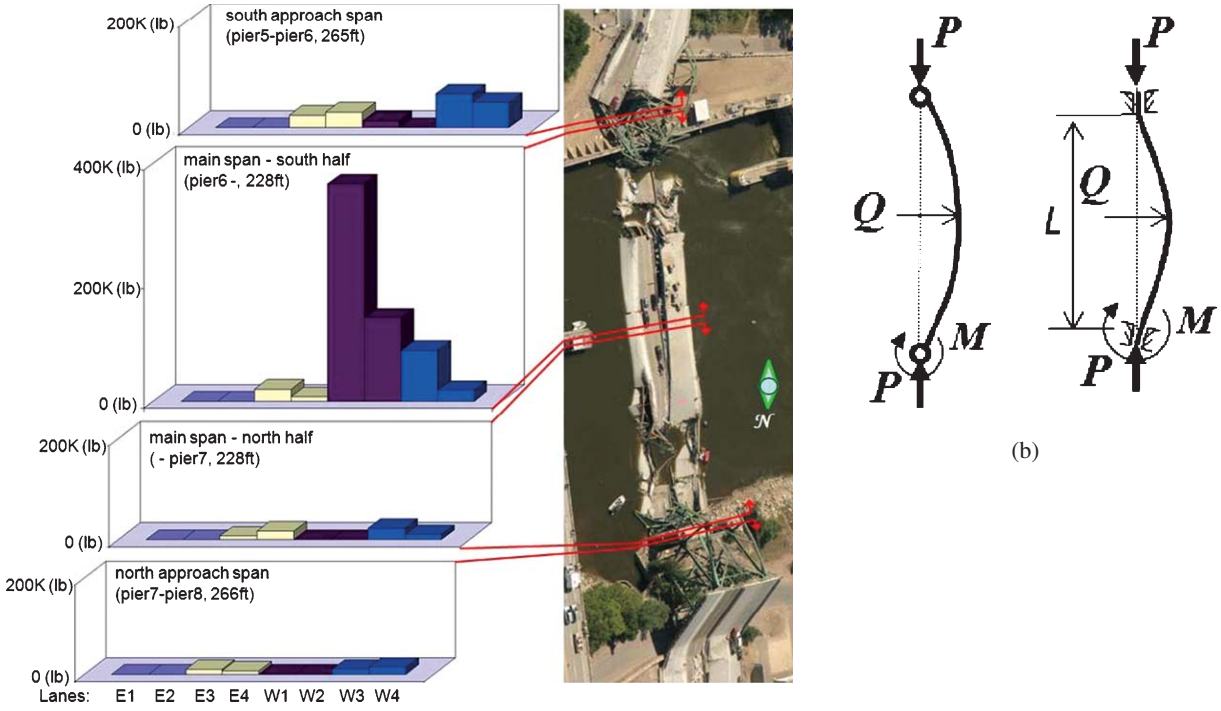

Fig. 19. (a) I35 W Bridge's deck live load distribution at the moment of collapse, which causes the difference Q_P in Fig. 18; (b) Eular's instability models with lateral force and bending moment under two boundary conditions; for gusset plate, the lateral force and bending moment are out-of-plan force and moment.

Figure 19(a) gives the deck load's distribution of the I35W Bridge when it collapsed. Although majority of the live loads laid on the western side, it should be noticed that the stock-piled construction materials, which is the heaviest part of total live-load, were on the lane W1 that is just beside the central line. This is the reason that the difference Q_P is less than 15% of the total force in the floor truss diagonal. Obviously, there is no need to address the fact that the deck load-induced vertical force on the western gusset plate is much higher than that on the eastern main flame. In Fig. 19(a) the live-load on the lane W1 equals the weight of several design trucks (80 kips each). In practical application, a worst scenario could be the case that multiple presence of heavy trucks line on one side of a bridge's deck, for example, the lane W4 in Fig. 19(a). Under this situation, Q_P can be significantly higher.

The forces Q_P and Q_D represent eccentric effect, caused by eccentric deck's live load and original design. They introduce extra out-of-plane forces and bending moment to a gusset plate, which may have significant impact to the plate's stability. For an engineering evaluation, conventional procedure often simplifies a structure into a one-dimensional model, then applying Eular's instability criterion, as illustrated in Fig. 19b. This criterion is exact for long slender structures such as bars and columns. For a two-dimensional structure like a gusset plate, Eular's criterion is generally over-conservative when all external forces lie in the same plane as the plate does. However, for either a one-dimensional bar or a two-dimensional plate, when lateral force or out-of-plane bending presents, see Fig. 19b, corresponding modifications are necessary. Theoretical solutions of lateral forces have already been obtained for one-dimensional bar, for examples, see [3, 8]. Theoretical analyses in these literatures indicate that, when an out-of-plane force Q or bending moment M is proportional to in-plane compression force P, for an elastic slender structure component the following relationship holds:

$$M_{\max} \propto \frac{P^2}{1 - \frac{P}{P_E}} \tag{1}$$

where $M_{\max}$ is the maximum bending moment in the component; P_E is the Eular's prediction of the load at

onset of instability. This relationship implies that a lateral load does not affect instability criterion under elastic condition. However, the maximum bending moment in the structure may increase faster because it is proportional to the square of in-plane load. This may cause material's yielding earlier than the case without out-of-plane forces, resulted in reduction of system stiffness and subsequent loss of stability even when applied load is still lower than Eular's prediction [26, 36].

A thin-plate theory-based model has been developed which partitions a gusset plate into several zones characterized by different failure modes [49a] and the model enables to obtain analytical or semi-analytical solution for each mode, as outlined in [49b]. For buckling, a group of semi-analytical solutions has been obtained based on Von Karman's thin plate stability theory [50]. Introductions of this theory and related applications can be found, for examples, in [3, 5, 8]. Further theoretical developments of structural stability can be found, for examples, in [21, 26, 27, 36]. According to this theory, the stability of this fan-shaped is governed by the stationary solution of the following equilibrium condition (in polar coordinate system)

A gusset plate can be treated as "thin plate" because its largest unbraced dimension is generally one order greater than its thickness. Such a thin plate may fail through two mechanisms: tension-induced material failure or buckling under compression, as discussed early in this paper. Accordingly, the two cases in Fig. 16 demonstrate the three corresponding patterns: (i) buckling at unbraced area due to the large ratio of the clearance between attached beams and the plate's thickness, Fig. 15c; (ii) compression-induced bowing of the triangle area of a gusset, Fig. 16a; (iii) tension induced necking in another triangle area of the gusset, together with shear failure around rivets, Fig. 16b. These patterns may occur concurrently or a dominant one triggers another. The challenges for design and load-rating a gusset plate are to identify the key dimension-parameters that are able to characterize geometric complexities and to compute the limit load at critical conditions considering lateral perturbation.

After some additional geometric modifications to the Whitemore model, a group of semi-analytical solutions of gusset plates' buckling has been obtained based the theory in [3, 8] and the Von Karman's thin plate stability criterion [50]. Introductions of this theory and related applications can be found, for examples, in [3, 5, 8]. More advanced theoretical developments of structural stability, including elastoplastic buckling, post buckling, imperfection sensitivities, can be found, for examples, in [21, 26, 27, 36]. According to this class of theories, the elastic stability of this fan-shaped plate is governed by the stationary solution of the following equilibrium condition (in polar coordinate system):

$$K\Delta\Delta w = N_{rr}\frac{\partial^2 w}{\partial r^2} + N_{\theta\theta}\left(\frac{\partial w}{r\partial r} + \frac{\partial^2 w}{r^2\partial\theta^2}\right) - 2N_{r\theta}\left(\frac{\partial w}{r^2\partial\theta} - \frac{\partial^2 w}{r\partial\theta\,\partial r}\right) \quad (2)$$

where N_{rr}, $N_{\theta\theta}$, $N_{r\theta}$ denote in turn the in-plane radial, hoop, and shear force densities; w is out-of-plane displacement; and K is plate stiffness:

$$K = \frac{Eh^3}{12(1-\upsilon^2)} \quad (3)$$

The solved force, normalized to the dimension of stress, is plotted in Fig. 20. A brief introduction of the "Modified Whitemore Model" is given in [18].

7. Conclusions

- To avoid a progressive collapse that occurred in I35W Bridge, an additional safety factor for ASD-Allowable Stress Design (or η_R in LRFD) may be necessary or those key single load-path structural members in a multi-span bridge when the bridge's design is merely based on the one-dimensional

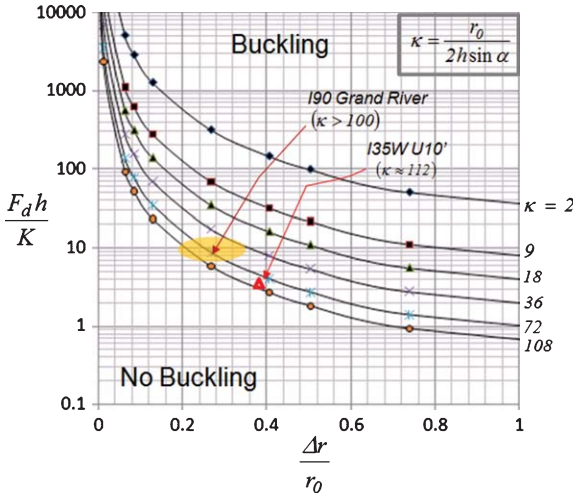

Fig. 20. A semi-analytic solution of gusset buckling based on Von Karman's thin plate instability theory[50]. For a given geometric parameter κ, each curve in this chart defines the corresponding critical load at buckling for a modified Whitmore mode [18]; F_d: the critical load at buckling.

influence-line analysis like that in Fig. 9(c).

- Roller bearing condition is crucial for maintaining an aged bridge's safety operation. Corrosion or other deterioration induced roller bearing lock may result in significant thermal stresses in a bridge.
- Stress concentration and bending moment: bending moment and induced-stress concentration around truss-joints may have remarkable effect on load capacity and fatigue life of truss-structured bridges. Due to the limited computational means in past, these effects might be treated in an *ah hoc* way, for example, enlarged safety factor. In order to avoid over-conservative or risky designs, relatively accurate computation may be necessary.
- Evaluation of gusset plates' load capacity: the results of the finite elements computation of I35W Bridge's superstructure and gusset plates suggest three failure modes of gusset plates, i.e. buckling, bowing, and tension; the latter equals shear failure for ductile steels. Both eccentric deck's live load and an inappropriated design of the joint between deck floor truss and main trusses frames will cause out-of-plane force and bending moment. These kinds of lateral forces may significantly reduce the critical load of a gusset plate's buckling due to localized nonlinear effects. Based on the theories introduced in [3, 8] and Von Karman's thin plate stability formulation [50], a semi-analytical solution for a modified Whitmore model of gusset plate has been discussed. However, for broad applications, more detailed analysis and comparisons with 3D numerical computations and experimental results may be necessary.

Acknowledgments

The author would like to express his appreciations to Mr. Foster, Mr. Bagnard, Mr. Wildey, Mr. Collions (NTSB), Mr. M. Lwin, Mr. E. Wasserman, Mr. M. Kerley, Dr. Ian Friedland, Dr. B.V. Johnson, Mr. C. Puzey, Mr. R. Pratt, Mr. H. Capper, Mr. N. McDonald, Mr. A.P. Yannotti, Mr. K. Thompson (AASHTO), Prof. T. Galambos (UM), Prof. Z. Bazant and Prof. J. Shofer (NWU), Prof. T. Oden (UTX) for the discussions in past two years. The author thanks Northwestern University Library for the convenience provided during this research. Mr. M. Lwin of FHWA and Mr. Ed. Wasserman of AASHTO T14 have reviewed the manuscript and provided valuable suggestions. The author would like to sincerely thank them again for their advice and encouragement for the work presented in the manuscript.

References

[1] M. Bagnard, *Gusset Plate Inspection Issues*, Presentation, Nov. 2008.
[2] K.-J. Bathe, *Finite Element Procedure*, Prentice-Hall Inc., 1996.
[3] B. Bazant, *Stability of Structures: Elastic, Inelastic, Fracture, and Damage Theories*, Mineola, Dover Pub, 2001.
[4] T. Belytschko, W.K. Liu and B. Moran, *Nonlinear Finite Elements for Continua and Structures*, John Wiley & Sons, New York, 2000.
[5] F. Bloom and D. Coffin, *Handbook of Thin Plate Buckling and Postbuckling*, Chapman and Hall/CRC, 2000.
[6] J.W. Fisher, *Fatigue and Fracture of Steel Bridges*, Wiley Interscience pub, 1984.
[7] D. Frangopol, et al., Multi-criteria optimization of life-cycle maintenance programs using advanced modeling and computational tools, in: *Trends in Civil and Structural Computing*", Chpt. 1, Saxe-Coburg Publications, 2009.
[8] G.V. Theodore, *Structural Stability of Steel Concepts and Applications for Structural Engineers*, John Willies & Son, 2008.
[9] K.W. Gee, "Load-carrying Capacity Consideration of Gusset Plates in Non-load-path-redundant Steel Truss Bridges", *FHWA Technical Advisory T 5140.29*., Jan. 15, 2008. FHWA, Washington, D. C., 2008.
[10] A.L. Gurson, Continuum Theory of Ductile Rupture by Void Nucleation and Growth: Path I-Yield Function and Flow Rules for Porous Ductile Media, *J Eng Mat Tech* **99** (1977), 2–17.
[11] S. Hao, "A Note of I35 W Bridge Collapse", ASCE, J. Bridge Engineering, Sept/Oct, 2010, pp. 608–618.
[12] S. Hao and W. Brocks, The gurson-tvergaard-needleman-model for rate and temperature-dependent materials, *Computational Mechanics* **20** (1997), 34.
[13] S. Hao, W.K. Liu, G.B. Olson and B. Moran, Multi-scale constitutive model and computational framework for the design of ultra-high strength, high toughness steels, *Computer Method in Applied Mechanics and Engineering* **193**(17–20) (1908), 1865–1908.
[14] S. Hao, I-35 W Report I, submitted to NTSB at 9/22/2007. http://www.suhao-acii.com/files/Report_SuHao_Sep22_2007
[15] S. Hao, I-35 W Reprot IV: A Complete Load Rating of I35 W Bridge (Submitted to NTSB at May, 2009).
[16] S. Hao, *Why the Gusset Plates of I-35 W Bridge Are Undersized?*, submitted to NTSB at 3/6/2008. http://www.suhao-acii.com/files/Report2_March2008.pdf
[17] S. Hao, A. Cornec and K.-H. Schwalbe, Engineering treatment model (ETM) for crack driving force estimation of structures with stress concentration, ASME, *Trans, J Pressure Vessels Tech* **115** (1993), 164–170.
[18] S. Hao, Proceedings of the ASME (American Society of Mechanical Engineers) Annual Congress 2010, November 12-18, 2010, Vancouver, paper number IMECE2010-38312.
[19] S. Hao and W.K. Liu, Moving particle finite element method with superconvergence: Nodal integration formulation and applications, *Computer Method in Applied Mech and Eng* **196** (2006), 6059–6072.
[20] R. Hill, *Mathematic Theory of Plasticity*, Oxford University Express, 1951.

[21] R. Hill and J.W. Hutchinson, Bifurcation phenomena in the plate tension test, *J Mech Phys Solids* **25** (1875), 239–264.
[22] R. Holt and J. Hartmann, *FHWA, Turner-Fairbank Research Center Report*, Jan. 12, 2008.
[23] A. Huckelbridge, D. Palmer and R. Snyder, Grand gusset failure, *Civil Engineering Magazine*, Sept. 1997.
[24] T.J.R. Hughes, *The Finite Element Method*, Prentice-Hall, New Jersey, 1987.
[25] J.W. Hutchinson, Singular behavior at the end of a tensile crack in a hardening material, *J Mech Phys Solids* **16**(1) (1968), 13–31.
[26] J.W. Hutchinson and W.T. Koiter, Postbuckling theory, *Appl Mech Rev* **23** (1970), 1353–1366.
[27] J.W. Hutchinson, M.Y. He and A.G. Evans, The influence of imperfections on the nucleation and propagation of buckling driving delaminations, *J Mech Phys Solids* **48** (2000), 709–734.
[28] F. Ibrahim, *Load Rating Evaluation of Gusset Plates in Truss Bridges*", FHWA, Feb. 2008.
[29] K. Ravi-Chandar and W.G. Knauss, An experimental investigation into dynamic fracture – IV", on the interaction of stress waves with propagating cracks, *International Journal of Fracture* **26** (1984), 189–200.
[30] H. Liebowitz (ed.), *Fracture, An Advanced Treatise*, Academic Press, New York, 1968.
[31] E. Maragakis, B.M. Douglas and C. Qingbin, Full-Scale Field Capacity Tests of a Railway Bridge.
[32] D.L. McDowell, K.A. Gall, M.F. Horstemeyer and J. Fan, *Eng Frac Mech* **70** (2003), 49–80.
[33] D.R. Mertz, Load and Load Combination, in: *Steel Bridge Design Handbook*, National Steel Bridge Alliance (NSBA), Chicago, Illinois, 2006.
[34] National Transportation Safety Board (NTSB), "Highway Accident Report Interstate 35 W Collapse Over the Mississippi River Minneapolis, Minnesota, August 1, 2007", *NTSB/HAR-08/03, Nov. 14, 2008*, NTSB, Washington, D.C.
[35] National Transportation Safety Board (NTSB), Safety Recommendation (H08-1), Jan. 15, 2008, Washington, D.C.
[36] A. Needleman, Postbifurcation behavior and imperfection sensitivity of elastic-plastic circular plates, *Int J Mech Sci* **17** (1975), 1–13.
[37] A. Needleman, A continuum model for void nucleation by inclusion debonding, *J Appl Mech* **54**(3) (1987), 525–531.
[38] NTSB, *Data Report: State-by-State Bridge Counts*, J.M. Price ed., March. 12, 2008.
[39] J.T. Oden, *Finite Elements of Nonlinear Continua*, McGraw-Hill Book Company, New York, 1972.
[40] J.N. Reddy, *Mechanics of Laminated Composite Plates and Shells. Theory and Analysis*, 2 nd ed., CRC Press, Boca Raton, FL, 2004.
[41] R.L. Reid, The infrastructure crisis, *Civil Engineering Magazine*, January, 2008.
[42] J.R. Rice and N. Levy, A line-spring model for surface crack, *J Appl Mech* **39**(1) (1972), 185–191.
[43] J.E. Rice and G.F. Rosengren, Plan strain deformation near a crack tip in a power-law hardening material, *J Mech Phys Solids* **16**(1) (1968), 1–12.
[44] J.R. Rice and D.M. Tracey, On the ductile enlargement of voids in triaxial stress field, *Journal of the Mechanics and Physics of Solids* **17** (1969), 2–15.
[45] K.-H. Schwalbe and A. Cornec, The engineering treatment model (ETM) and its practical application, *Fatigue Fract Enyn 9 Mat, Struct*, **14** (1991), 405–412.
[46] E. Sternberg and G.C. Lee, Meeting the challenge of facility protection for homeland security, *J Homeland Security and Emergency Management*, February 2006.
[47] S. Sureash, *Fatigue of Materials*, 2nd edn., Cambridge University Press, 1998.
[48] S.P. Timoshenko and J.N. Goodier, *Theory of Elasticity*, McGraw-Hill, 1970.
[49] V. Tvergaard, *On Localization in Ductile Materials Containing Spherical Voids*, *Int J Fract* **18** (1982), 237–252.
[50] T. Von Karman, Festigkeitsprobleme im Maschinenbau, in: *Encylop¨adie der Mathematischen Wissenschaften*, IV/4C, 1910, 311–385.
[51] R.E. Whitmore, *Experimental Investigation of Stresses in Gusset Plates*, Bulletin No. 16, Engineering Experiment Station, University of Tennessee, 1952.
[52] O.C. Zienkiewicz and R.L. Taylor, *The Finite Element in Engineering Science,* McGraw Hill, 1972.